ICES Journal of Marine Science, 62: 956–965 (2005)
doi:10.1016/j.icesjms.2005.01.024

Broad-bandwidth, sound scattering, and absorption from krill (*Meganyctiphanes norvegica*), mysids (*Praunus flexuosus* and *Neomysis integer*), and shrimp (*Crangon crangon*)

Stéphane G. Conti, David A. Demer, and Andrew S. Brierley

Conti, S. G., Demer, D. A., and Brierley, A. S. 2005. Broad-bandwidth, sound scattering, and absorption from krill (*Meganyctiphanes norvegica*), mysids (*Praunus flexuosus* and *Neomysis integer*), and shrimp (*Crangon crangon*). – ICES Journal of Marine Science, 62: 956–965.

Sound scattering and absorption by Northern krill (*Meganyctiphanes norvegica*) were measured over the acoustic bandwidth of 30–210 kHz and compared with similar scattering measurements for Antarctic krill (*Euphausia superba*). The measurements of total target strength (TTS; energy scattered in all directions, averaged over all angles of incidence) match the SDWBA model (stochastic distorted-wave Born approximation) recently developed for Antarctic krill, indicating its validity for other euphausiid species with similar size and shape. However, the TTS of crustaceans with markedly different shapes are not well predicted by SDWBA derived with the generic krill shape and scaled to animal length (L). Therefore, crustacean target strength (TS) may not be estimated accurately by a linear function of $\log_{10}$(L), irrespective of shape, questioning the validity of the current TS relationship used for Antarctic krill derived from data measured from multiple crustaceans. TTS and TS are dependent upon both L and shape, and different crustaceans have significantly different shapes and width-to-length relationships. In contrast, modelled TTS and TS spectra for gravid and non-gravid krill appear to have differing amplitudes, but similar shapes. Additionally, measurements of absorption spectra from decapods indicate that the absorption cross-section increases with the volume of the animal.

Keywords: acoustic scatter, Born approximation model, distorted-wave, modelling, stochastic, total cross-section, total target strength.

Received 1 November 2004; accepted 10 January 2005.

S. G. Conti and D. A. Demer: Southwest Fisheries Science Center, 8604 La Jolla Shores Drive, La Jolla, CA 92037, USA. A. S. Brierley: Gatty Marine Laboratory, University of St Andrews, Fife KY16 8LB, Scotland, UK. Correspondence to S. G. Conti: tel: +1 858 546 5603; fax: +1 858 546 5652; e-mail: stephane.conti@noaa.gov.

Introduction

Knowledge of the abundance and distribution of species is among the most basic requirements for understanding ecosystem function and for the management of living resources. In the marine environment, pelagic organisms such as commercially and ecologically important fish, micronekton, and zooplankton can be sampled with nets, but acoustic-survey techniques are advantageous because they permit continuous and non-destructive sampling over larger areas in shorter periods of time. The abundance and distribution of Antarctic krill (*Euphausia superba*), for example, are routinely determined by acoustic surveys (e.g. Brierley *et al.*, 1999; Hewitt *et al.*, 2004).

Accurate target strength (TS) information is fundamental to the interpretation of acoustic-survey data. TS describes the portion of incident acoustic energy that is scattered from an individual fish or zooplankton. It is dependent on acoustic frequency, and the animal's size (length and volume), shape, orientation, and material properties. Although TS is highly sensitive to these variables, they have of necessity been largely ignored in the analysis of acoustic-survey data. TS can be estimated in a number of ways including the direct ensonification of tethered individuals, i.e. confined within the usually narrow echosounder beam (Stanton *et al.*, 1998), *in situ* observations (Warren *et al.*, 2001), and modelling (Foote, 1991; Ona, 1999). Although there have been numerous recent

1054-3139/$30.00

advances in the direct acoustic observation of zooplankton TS (e.g. McGehee *et al.*, 1998; Brierley *et al.*, 2004), for logistical reasons most studies have been restricted to one species and narrow ranges of frequency, organism size, and maturity stage. For example, the TS/length relationship for Antarctic krill presently used (Greene *et al.*, 1991; Hewitt *et al.*, 2004) does not take account of the maturity stage of the animal. A gravid adult female of 55 mm standard length has a mass 9.5% greater than a mature male of the same length (Morris *et al.*, 1988) but both are assumed to have the same TS. This shortcoming contributes to uncertainty in acoustic estimates of krill abundance.

Recently, a method has been developed for estimating the total scattering cross-section σ_T from scatterers in motion, like marine organisms (total target strength $TTS = 10\log_{10}\left(\frac{\sigma_t}{4\pi}\right)$; de Rosny and Roux, 2001). TTS represents the acoustic energy scattered from an object in all directions, averaged over all angles of incidence. TS is closely related to TTS, but while TS is a function of many different variables (e.g. animal size, shape, orientation), this measurement technique conveniently provides accurate and precise measurements of broad-bandwidth TTS (Demer *et al.*, 2003). Application of the technique to live, free-swimming organisms can provide improved TS information leading to substantial improvements in the at-sea acoustic identification and assessment of ecologically and commercially important pelagic species (Conti and Demer, 2003; Demer and Conti, 2003a). This is possible because physics-based scattering models validated using TTS measurements can be used to predict TS at different angles of incidence, or averaged over an applicable distribution of angles (Demer and Conti, 2005).

In this study, the TTS technique is used to measure the broad-bandwidth sound scatter from Northern krill (*Meganyctiphanes norvegica*) and compared with similar measurements made on Antarctic krill (*Euphausia superba*). These euphausiid species have similarities in their shapes and maturity stages, have overlapping length distributions, and are key species in the North Atlantic and Southern Ocean ecosystems, respectively. Proof of equivalence in their broad-bandwidth sound scattering characteristics will expand the opportunities to improve the accuracy of TS estimation and aid in the acoustic identification and survey of both species. For example, convenient access to the shorter-lived *M. norvegica* could allow broad-bandwidth TTS measurements to be made rapidly over a variety of maturity stages. This, in turn, could lead to a reappraisal of the TS relationship used internationally for Antarctic krill, and could thus provide an indication of the likely error resulting from the effective dismissal of shape and maturity stage differences in conventional euphausiid TS (Greene *et al.*, 1991). We also present TTS measurements for mysids and decapod shrimp. Data from these taxa were used by Greene *et al.* (1991) in their determination of TS for Antarctic krill. However, their different gross anatomical shapes make the use of these data perhaps questionable.

Also presented are the first measurements of absolute sound absorption from marine crustaceans. The absorption measurement technique employed here was first described by Conti *et al.* (2004) and led to the measurement of the absorption cross-section $\sigma_a\left(ABS = 10\log_{10}\left(\frac{\sigma_a}{4\pi}\right)\right)$. These measurements add to the study of sound propagation in the presence of krill.

Methods

From 1 to 8 August 2003, TTS and ABS measurements of krill (*Meganyctiphanes norvegica*), mysids (a mix of *Praunus flexuosus* and *Neomysis integer*), and shrimp (*Crangon crangon*) were made at the Scottish Association of Marine Sciences' Dunstaffnage Marine Laboratory, Oban, Scotland. Details of the general processing steps are outlined in de Rosny and Roux (2001), Demer *et al.* (2003), Demer and Conti (2003a), and Conti *et al.* (2004). Equipment and analysis steps specific to these experiments follow.

The krill were captured in Loch Etive, Scotland, in the deep holes to the southeast of Bonawe quarries using a 1-m diameter hoop net. The net was towed horizontally from RV "Seol Mara" at various depths ranging from approximately 120 m during the daytime to approximately 60 m at night. The mysids were captured in a shallow embayment to the south of the Marine Laboratory in Dunstaffnage Bay using a hand net. The shrimp were captured in Tralee Bay at low tide by hand-dragging a 2-m long beam trawl. The krill and shrimp were kept alive and transferred to the laboratory in 20-l insulated containers and stored temporarily in aquaria. The mysids were captured immediately prior to making the measurements and stored briefly in buckets.

For each experiment, a 20-l stainless-steel bucket was filled with 17 l ($\pm$1%) of ambient seawater at temperatures ranging from 13.8 to 14.2 °C. Groups of live swimming animals were then added sequentially (Figure 1).

Four sets of frequency-modulated pulses (1.0 $V_{p\text{-}p}$; 18 ms pulse length) with overlapping bandwidths (30–90, 80–130, 120–170, and 160–210 kHz, centre frequencies f_c of 60, 105, 145, and 185 kHz, respectively) were generated (Hewlett Packard 33120A arbitrary waveform generator), amplified 20 dB (Krohn-Hite 7500 power amplifier), and transmitted once per second using an omni-directional, broad-bandwidth emitter (ITC 1042) and received bi-statically with two omni-directional, broad-bandwidth receivers (ITC 1042 and Reson TC4013). The emitter and two receivers were suspended in the tank via aluminium rods attached to the top of the bucket (Figure 1). For each bandwidth, ensembles of 100 pulses were transmitted, and the reverberation time-series $h_k(t)$ (where k is the pulse number) were recorded over 70 ms and digitized at 500 kHz, using a 12-bit analog-to-digital converter (National Instruments DAQPad 6070E).

To reduce noise and align the time of origin for all frequencies, the $h_k(t)$ were match-filtered via cross-correlations with their respective transmitted signals. The coherent intensity ($\langle h_k(t)h_{k+1}(t)\rangle$) in the 100-pulse ensembles identified sound scattered from the echoic bucket. Because the positions of the animals were uncorrelated from ping-to-ping, the incoherent intensity ($\langle h_k(t)^2\rangle$) described sound scattering from the animals. The ratio of coherent and incoherent intensities decayed exponentially:

$$S(t) = \left[\frac{\langle h_k(t)h_{k+1}(t)\rangle}{\langle h_k(t)^2\rangle}\right] \approx \exp\left(-tc\frac{n\sigma_t}{v}\right), \quad (1)$$

where σ_t is the total scattering cross-section of one animal, v the volume of the cavity, n the number of animals, c the speed of sound in seawater, $\langle\rangle$ designated the average taken over the pings, and [] the average taken over the experiments for the same group of animals (i.e. runs with different positions of the emitter and receivers).

The exponential decay of S(t) was estimated for each 100-pulse ensemble by low-pass filtering the numerator and denominator ($f_{cutoff} = 0.016 \times f_{sampling}/2$), and fitting a slope ($d\ln(S(t))/dt$) in the least-squares sense, while requiring $5 \leq t \leq 20$ ms and forced through the origin ($\ln(S(t = 0)) = 0$). Knowing the volume of the cavity (v), the number of animals (n), and the speed of sound in seawater (c), an estimate of σ_t was made for each group of animals and bandwidth:

$$\sigma_t \approx -\frac{v}{cn}\frac{d\ln(S(t))}{dt}. \quad (2)$$

The σ_T calculated from the data was then converted to TTS as a function of frequency.

Figure 1. Northern krill swimming in a 17 ± 1%-l stainless-steel bucket (Vollrath 58200). Aluminium rods were used to suspend the omni-directional emitter (ITC 1042), and two omni-directional receivers (ITC 1042 and Reson TC4013), and a thermocouple near the centre of the water volume.

Thus, TTS(f) measurements were made from the reverberation sensed at two receiver locations, and during multiple 10-min runs. In total, measurements were made of two aggregations of 115 and 135 non-gravid swimming krill; five aggregations of 50–75 gravid and non-gravid shrimp (Table 1); and three aggregations of 1055, 1479, and 2256 gravid and non-gravid mysids. In order to prevent animals aggregating at the side of the tank, which they did in daylight presumably in an attempt to avoid light (Figure 1), the measurements were performed in the dark. Following the measurements of each aggregation, the length of each animal L, viz. from the anterior tip of the rostrum and the posterior end of the uropods, excluding their terminal setae (Figure 2), was measured to the nearest millimetre before it was preserved in sample jars with 4% buffered formaldehyde. To predict the empirical estimates of σ_t, the SDWBA model (Demer and Conti, 2003b) was run to obtain $SDWBA_{TTS}$. The computations are detailed in Demer and Conti (2003a). Parameters include a shape with width-to-length ratio 1.4 times that of the generic krill shape from McGehee *et al.* (1998), $c = 1455\ m\ s^{-1}$, the non-dimensional speed of sound and density contrasts ($h = 1.0279$ and $g = 1.0357$) from Foote *et al.* (1990) and Foote (1991), respectively. The random phase was chosen from a normal distribution ($\varphi = N[0, 40.5°]$) from Demer and Conti (2003a). The generic krill shape, which was derived from a starved krill with $L = 38.35$ mm, was scaled proportionately to represent the larger krill in these experiments (average $L = 36.35$ mm). Thus, $SDWBA_{TTS}$ was evaluated from 30 to 210 kHz.

The absorption cross-sections (σ_a) of the krill, shrimp, and mysids were measured using the same experimental setup, and the technique outlined in Conti *et al.* (2004). Prior to the introduction of the animals in the bucket, the reverberation time-series for the empty bucket $h_{k\,empty}(t)$ were recorded multiple times for the same position of the emitter and receivers. Then the animals were introduced into the bucket without moving the emitter and receivers, and the reverberation time-series $h_k(t)$ were recorded with the animals swimming. The incoherent intensity for the empty bucket and the bucket with the animals swimming are compared, and the ratio decays exponentially:

Table 1. The parameters of the groups of shrimp for the absorption measurements.

Number of shrimp	L_{min}	L_{max}	Maturity
75	25	30	Mixed
75	30	35	Mixed
75	35	40	Mixed
75	40	45	Mixed
50	50	55	Gravid

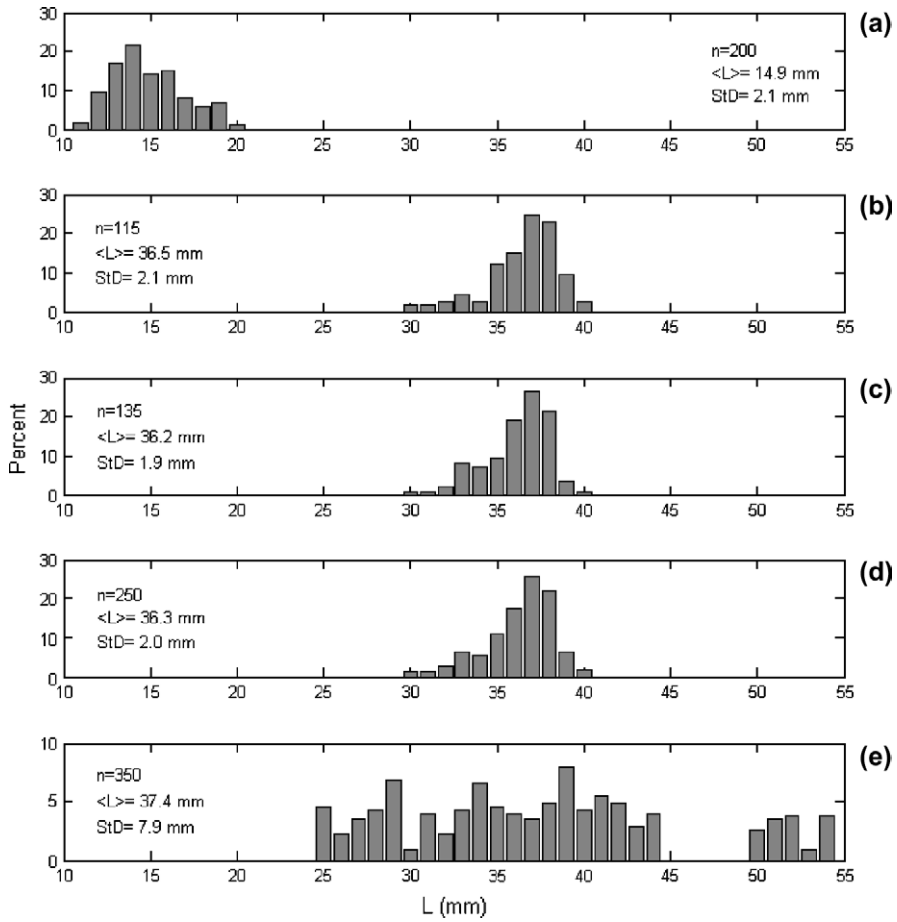

Figure 2. Length distributions of the mysids (a), 115 krill (b), 135 krill (c), combined krill (d), and the shrimp (e).

$$S_a(t) = \left[\frac{\langle h_k(t)^2\rangle}{\langle h_{k\,empty}(t)^2\rangle}\right] \approx \exp\left(-t\frac{cn\sigma_a}{v}\right). \quad (3)$$

Using the same low-pass filter as in the total scattering cross-section measurement, the absorption cross-section was obtained knowing the volume of the cavity (v), the number of krill (n), and the speed of sound in seawater (c):

$$\sigma_a \approx -\frac{v}{cn}\frac{d\ln(S_a(t))}{dt} \quad (4)$$

$$ABS = 10\log_{10}\left(\frac{\sigma_a}{4\pi}\right). \quad (5)$$

The addition of the animals slightly changes the volume of the tank but the modification is small. The overall absorption from the tank remains identical. However, the arrival times of the main echoes from the cavity may shift when the total volume changes between the recordings without and with the animals. This could lead to problems in estimating the ratio $S_a(t)$ because the times of zeroes from the main echoes for $\langle h_k(t)^2\rangle$ and $\langle h_{k\ empty}(t)^2\rangle$ may not correspond. This problem is compensated by using multiple recordings for the tank without and with animals to average the zeroes, and smoothing both $\langle h_k(t)^2\rangle$ and $\langle h_{k\ empty}(t)^2\rangle$.

The reverberation time-series recorded for each of the four experimental bandwidths provided the average values of the total scattering and absorption cross-sections over each bandwidth. The total scattering spectra $\sigma_T(f)$ were obtained by filtering the reverberation time-series in narrow bands. Between 30 and 90 kHz, the spectra were measured with a 6-kHz resolution. For the three bands spanning 80 to 210 kHz, the frequency resolution was 5 kHz. For the absorption measurements, only the average values for each of the four experimental bandwidths were obtained.

Results

The mean standard lengths of the two groups of 115 and 135 Northern krill were 36.5 (s.d. = 2.1) and 36.2

(s.d. = 1.9) mm, respectively. The mean TTS spectra of each group was measured (Figure 3). The TTS measurement precision (s.d.) was estimated from multiple measurements at each frequency as ±14% and ±12%, respectively. Over the entire measured bandwidth, the TTS measurements for the krill matched the $SDWBA_{TTS}$ model to better than 26% (1 dB). Multiple additional measurements were attempted with groups of 26–75 krill, but discarded because of low signal-to-noise ratios. Some measurement series were also discarded due to disturbances of the water/air interface, low signal-to-noise ratio, and water-temperature fluctuations during the acquisition. The TTS measurements with 115 and 135 krill were obtained from animals with similar lengths (Figure 2). Therefore, the TTS spectra normalized to one animal were similar in both cases. They compared favourably with the theoretical predictions derived and validated for Antarctic krill (Demer and Conti, 2003a).

The TTS measurements for the mysids and shrimp were made from groups of animals with different size distributions (Figure 2). The mysids were smaller than the krill, and the size distribution of the shrimp was broader. Neither the TTS spectra for the mysids nor the shrimp matched the SDWBA predictions derived with the krill shape and adjusted for length (Figure 4). This result is not surprising since each of the three species has significantly differing length-to-width relationships (Figure 5, Table 2) with those of shrimp and mysids being larger than that of the krill. Consequently, their TTS are approximately 100% and 200% higher than the theoretical predictions derived using a generic krill shape, respectively. The measurement precision for TTS of mysids and shrimp was estimated as ±20%.

The dorsal-aspect views and shapes of gravid and non-gravid krill show differences (Figure 6, and unpublished data from Tarling *et al.* — see acknowledgements). The abdomen for a gravid krill is larger than for a non-gravid one. Using the SDWBA model and the shapes of gravid and non-gravid northern krill both TTS and TS predictions were computed (Figure 7). These predictions for TTS show that the spectrum for a gravid krill is higher than for a non-gravid one, but despite the amplitude difference, the discrepancies in the animal shape do not modify the frequency response significantly. Compared with the predictions for Antarctic krill, the spectra are similar in amplitude, and a difference can be observed at low frequencies where the spectrum for Antarctic krill drops faster than for Northern krill mainly because the Northern krill are thinner than the Antarctic krill in the modelling. The TS show some discrepancies for the dorsal aspect, but these discrepancies tend to be smoothed when the TS is averaged for the different distribution of orientation angles found in the literature for krill (Kils, 1981; Endo, 1993; Demer and Conti, 2005).

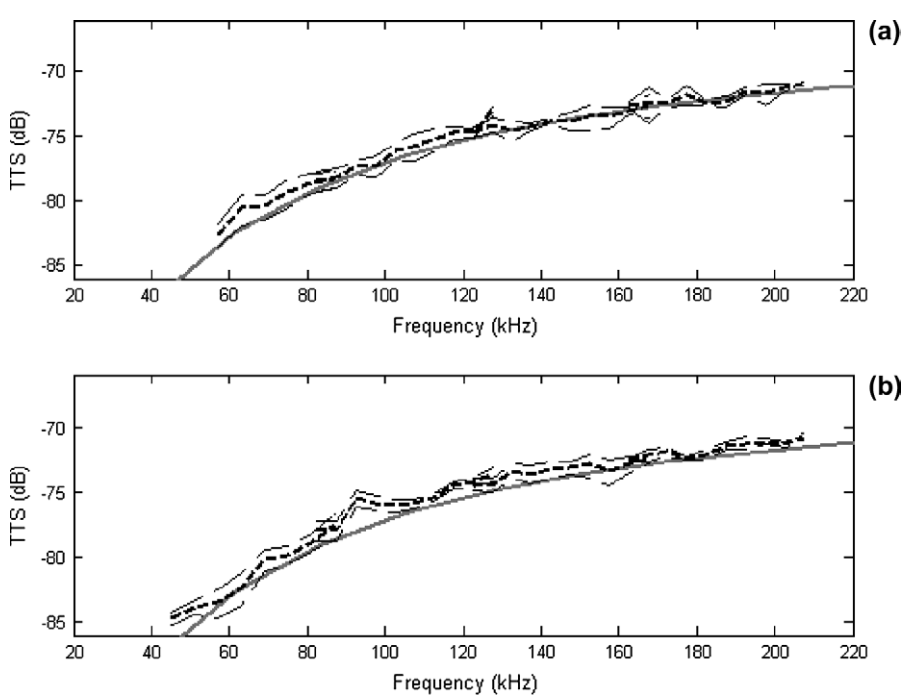

Figure 3. Mean TTS of *M. norvegica* measured from aggregations totalling 115 and 135 animals (bold dashed lines in a and b, respectively). For each run, the spectra were recorded with two hydrophones at different positions in the bucket. Standard deviations were calculated from three or four measurements from each aggregation and plotted (light dashed lines). The $SDWBA_{TTS}$ predictions (solid lines), were computed with g = 1.0357, h = 1.0279, generic shape, and the overall krill-length frequency distribution (see Figure 2).

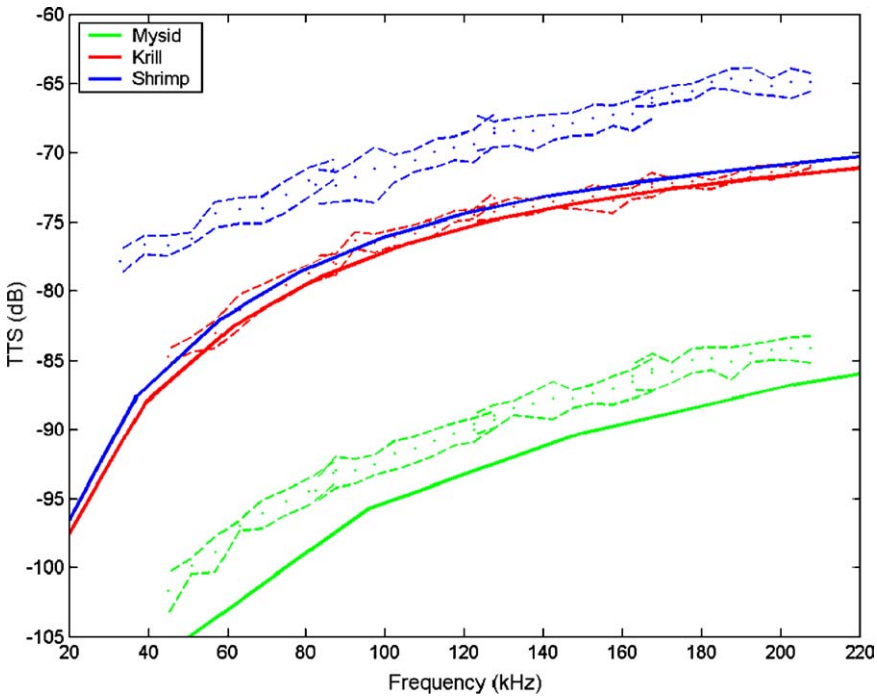

Figure 4. Broad-bandwidth mean TTS measurements of mysids, krill, and shrimp (green, red, and blue dots, respectively) with standard deviation (dashed lines), and predictions from the SDWBA model derived using a krill shape scaled to the mean length of each species (solid lines).

The absorption measurements at frequencies f_c were plotted against the animal length L for the krill, mysids, and shrimp (Figure 8). No relationship can be derived between ABS and L for the krill and mysids because of the small number of groups measured and their narrow length distributions. In comparison, the ABS measurements for shrimp were obtained from five different groups of gravid and non-gravid animals of different size (Table 1), and a relationship between ABS and L can be estimated (Figure 8, dark lines). It appears that the absorption cross-section of the shrimp increases in proportion to the animal volume ($\sigma_a \propto L^3$, $ABS = 30 \log_{10}(L) + C^{te}$), with relatively low residuals ($|R| \approx 3$). An absorption cross-section proportional to the area of the animal ($\sigma_a \propto L^2$, $ABS = 20 \log_{10}(L) + C^{te}$) gave higher residuals ($|R| = 3.84$, 4.97, 4.08, and 3.43 at 60, 105, 145, and 185 kHz, respectively). The similar relationship for the krill (Figure 8, light lines) suggests that the absorption for krill may also increase linearly with animal volume, but with a different proportionality constant.

Discussion

Because mysids and shrimp have markedly different body shapes and length-to-width ratios from those of euphausiids, the SDWBA model derived with the generic krill shape cannot be used to accurately predict the scattering from these crustaceans. Conversely, an empirical TS model derived from TS measurements of a variety of crustaceans, not including Antarctic krill, does not accurately predict TS for Antarctic krill (Demer, 2004; Demer and Conti, 2005). It is possible that the SDWBA model could predict accurately TS for mysids and shrimp, if it was evaluated using their specific shapes. Such analysis is beyond the scope of this study.

Because the TTS from both Northern and Antarctic krill support the SDWBA model derived with the same generic krill shape, there are now more opportunities to apply acoustic measurements of one species to the acoustic characterization of the other. For example, acoustic measurements of Northern krill can be used to improve the techniques for species delineation and target strength estimation for surveys of Antarctic krill.

SDWBA TS predictions show that the discrepancies in animal shape significantly modify the nulls and maxima for the dorsal-aspect backscattering. However, when TS spectra for gravid and non-gravid krill are averaged over the different distributions of animal orientation observed for krill, the nulls and maxima of each spectrum are smoothed, and the resulting frequency responses become more similar, despite significant differences in their amplitudes. Demer and Conti (2005) demonstrate that the distribution of orientations N(15°, 5°) is the most realistic one, and

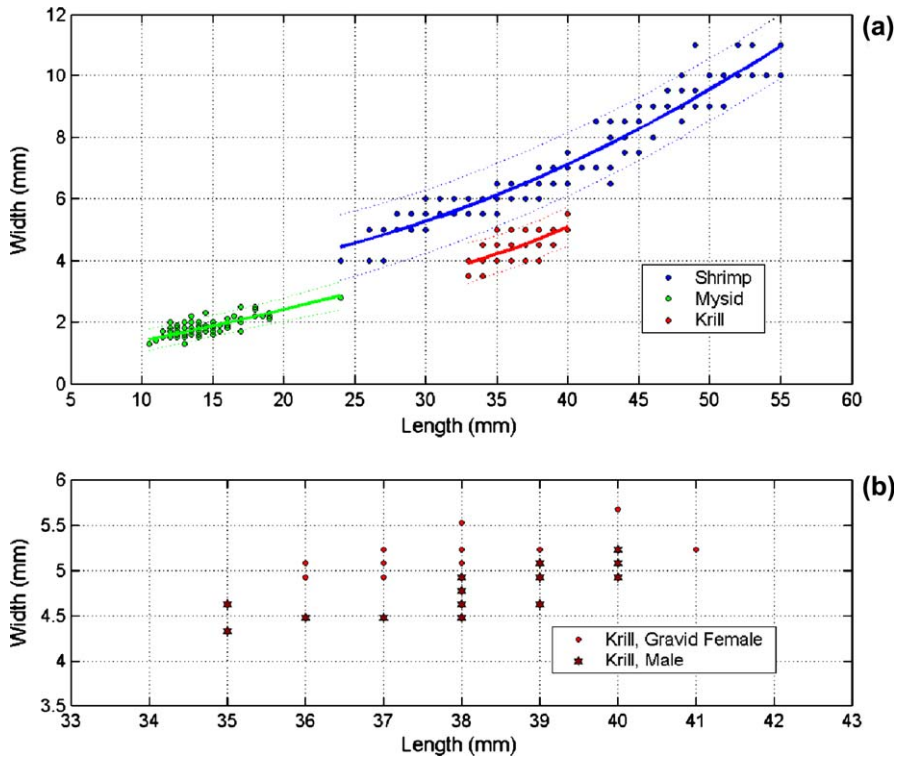

Figure 5. (a) Length-to-width relationships for shrimp (n = 117), mysids (n = 97), and krill (n = 97). The dashed lines indicate the 95% confidence intervals for the second-order polynomial fits (Table 2); the norms of the residuals R were 5.5, 1.6, and 2.9, respectively. The measurement precisions were ±1 mm for length and ±0.1 mm for width. The mysids included a mix of *Praunus flexuosus* and *Neomysis integer*. *P. flexuosus* is the larger of the species, potentially as long as 25 mm; *N. integer* can reach a maximum length of 17 mm. (b) Length-to-width measurements for gravid and non-gravid krill.

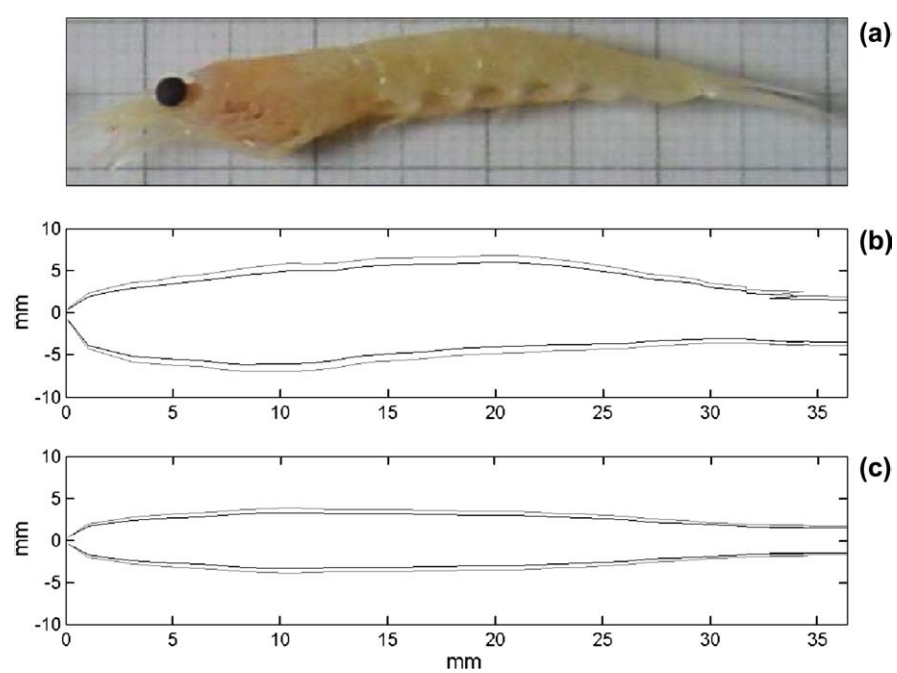

Figure 6. Side view of *Meganyctiphanes norvegica* (a), and non-gravid (dark) and gravid (grey) contours for the side (b) and dorsal (c) aspect used for the SDWBA predictions.

Table 2. The width-to-length, second-order polynomial parameters for krill, shrimp, and mysids ($W = A \times L^2 + B \times L + C$) and the corresponding norm of the residuals (R).

	A	B	C	R
Krill	5.475e−3	−0.2326	5.6291	2.9
Shrimp	2.873e−3	−0.0158	3.1493	5.5
Mysids	0.808e−3	0.0778	0.5225	1.6

corresponds to very similar frequency responses for the TS spectra of gravid and non-gravid krill, but still showing amplitude discrepancies. Since the spectra for gravid and non-gravid krill are expected to be similar, their respective proportions may not be estimated from acoustic measurements. However, knowing the relative proportions of gravid and non-gravid krill during the survey, from net sampling for example, the TS model used to analyse data from surveys can account for the proportion of gravid vs. non-gravid krill. Thus, a more accurate estimate of their total biomass may be obtained.

Conclusion

The results of this study underscore the importance of animal shape when modelling sound scatter from different species of crustacean zooplankton. It is shown that the SDWBA model can be used to accurately predict the sound scatter from both *Euphausia superba* and *Meganyctiphanes norvegica*, if their shapes are taken into account. Because Northern krill are generally more accessible to researchers, there are now more possibilities for studying changes in sound scatter from either Antarctic or Northern krill due to variations in their size, shape, and orientation.

For krill of the same species, the differences in shapes, of non-gravid and gravid specimens for example, may generate significant differences in the shapes and magnitudes of their respective frequency responses for the dorsal aspect, and should be taken into account when analysing survey data. These differences are smoothed though when averaged over a wide distribution of orientations. This is an important point because the empirical TS model commonly used to predict scattering from Antarctic krill is only valid

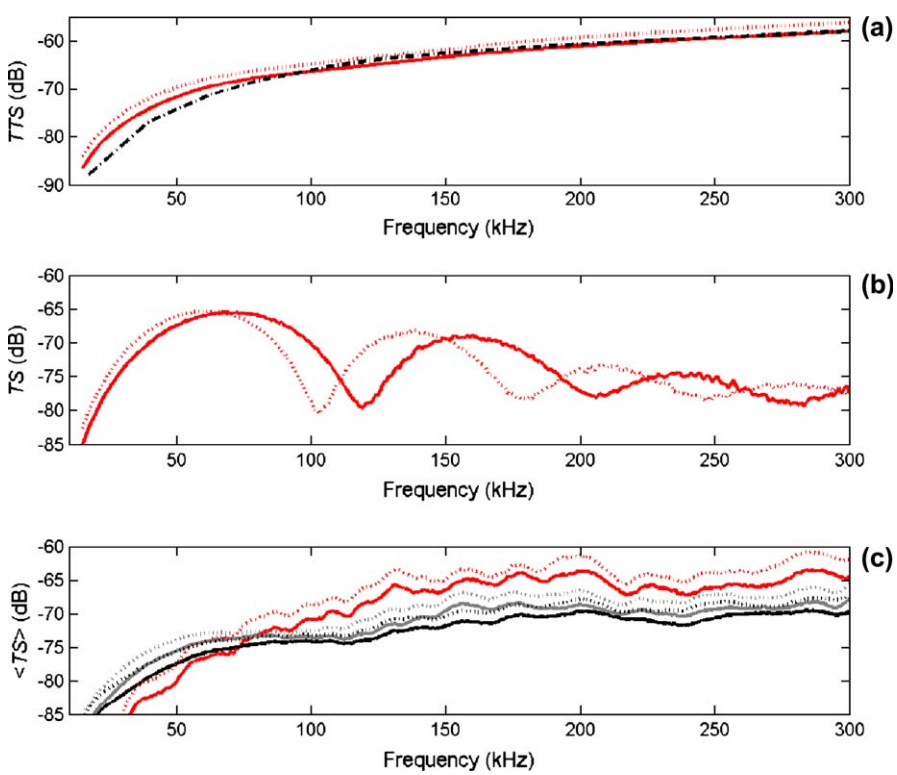

Figure 7. Comparison of SDWBA TTS and TS for non-gravid (solid red) and gravid (dashed red) *Meganyctiphanes norvegica*, length 36.35 mm (Tarling *et al.*, unpublished data, see acknowledgements). (a) The red lines correspond to the TTS for *Meganyctiphanes norvegica* gravid and non-gravid, and the dashed dark line to the TTS for *Euphasia superba* from Demer and Conti (2003a). (b) Dorsal-aspect TS for non-gravid (solid red) and gravid (dashed red) *Meganyctiphanes norvegica*. (c) TS for *Meganyctiphanes norvegica* averaged ($\langle TS \rangle$) for different orientation distributions of krill. The red lines correspond to the normal distribution of orientations N(15°, 5°) from Demer and Conti (2005). The dark and light lines correspond, respectively, to the normal distribution of orientations found in the literature for krill: N(44.3°, 19.6°) from Endo (1993) and N(44.7°, 30.4°) from Kils (1981).

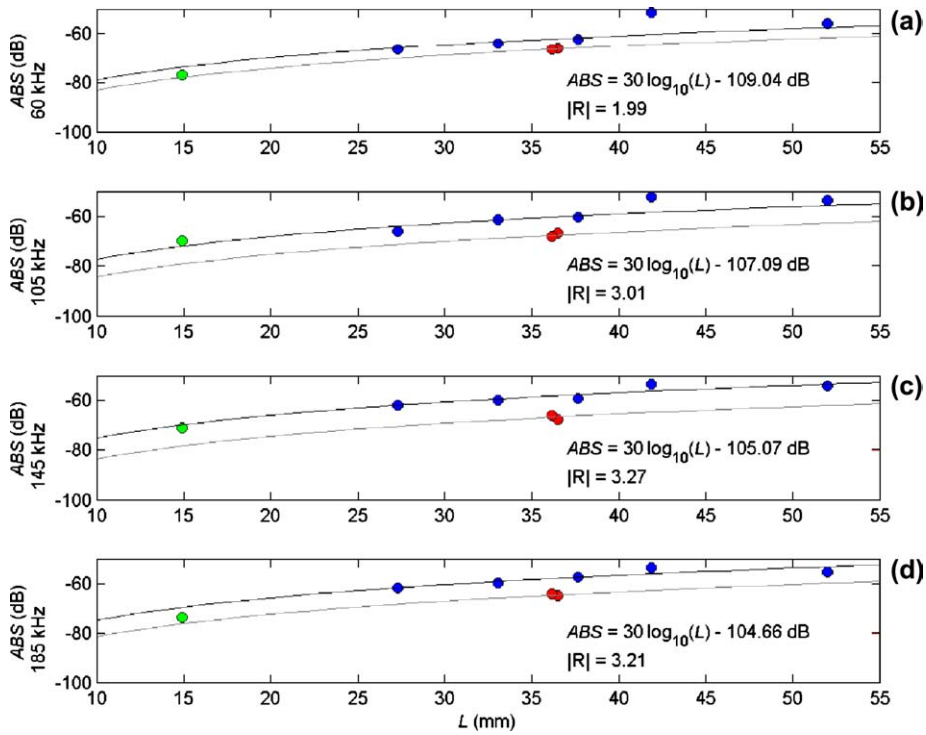

Figure 8. Absorption measurement vs. length L for the mysids (green dots), krill (red dots), and shrimp (blue dots), for each of four frequency bands f_c (a − 60 kHz, b − 105 kHz, c − 145 kHz, d − 185 kHz). The light curves correspond to 30 $\log_{10}$(L) for the krill. The dark curves correspond to 30 $\log_{10}$(L) fit for the shrimp data given by the equations and the corresponding norm of the residuals |R|.

in the geometric regime, does not take account of animal shape, and was derived from measurements of a variety of crustacean zooplankton, excluding Antarctic krill (Greene *et al.*, 1991). Moreover, the model of Greene *et al.* (1991) predicts that sound scatter from crustacean zooplankton is dependent on the animal's volume, essentially length cubed, whereas the SDWBA model predicts that TS is a function of cross-sectional area, essentially length squared. This difference is discussed in more detail in Demer and Martin (1995). It follows that the application of the empirical TS from Greene *et al.* (1991) to *Euphausia superba* may be inappropriate for multiple reasons. The measurements of absorption cross-section from shrimp indicate an L^3 proportionality approximately, or, in other words, volumetric dependence.

Acknowledgements

The measurements reported here were funded by a Small Grant from the UK's Natural Environment Research Council (NERC). Additional apparatus needed to be able to make them was funded by a Royal Society Research Grant whilst salary support came from the Fisheries Resources Division, SWFSC, NERC, and the University of St Andrews. Ship time and laboratory space were provided under a Scottish Association for Marine Science Bursary, and we thank the Director and staff of the SAMS Dunstaffnage Marine Laboratory for facilitating our visit. We thank R. Saunders for assistance with net sampling. Data on the ratio of krill thoracic width to total length were collected by G. Tarling, I. Everson, and B. Bergstorm, as part of an ARI funded project at Kristeneberg Marine Station, Sweden, investigating krill biomass and population dynamics in Gullmarsfjorden.

References

Brierley, A. S., Axelsen, B. E., Boyer, D. C., Lynam, C. P., Didcock, C. A., Boyer, H. J., Sparks, C. A. J., Purcell, J. E., and Gibbons, M. J. 2004. Single-target echo detections of jellyfish. ICES Journal of Marine Science, 61: 383−393.

Brierley, A. S., Demer, D. A., Watkins, J. L., and Hewitt, R. P. 1999. Concordance of interannual fluctuations in acoustically estimated densities of Antarctic krill around South Georgia and Elephant Island. Marine Biology, 134: 675−681.

Conti, S. G., and Demer, D. A. 2003. Wide-bandwidth acoustical characterization of anchovy and sardine from reverberation measurements in an echoic tank. ICES Journal of Marine Science, 60: 617−624.

Conti, S. G., Roux, P., Demer, D. A., and de Rosny, J. 2004. Measurement of the scattering and absorption cross-sections of the human body. Applied Physics Letters, 84: 819−821.

Demer, D. A. 2004. An estimate of error for the CCAMLR 2000 estimate of krill biomass. Deep Sea Research II, 51: 1237−1251.

Demer, D. A., and Conti, S. G. 2003a. Validation of the stochastic distorted-wave Born approximation model with broad-bandwidth total target-strength measurements of Antarctic krill. ICES Journal of Marine Science, 60: 625−635.

Demer, D. A., and Conti, S. G. 2003b. Reconciling theoretical versus empirical target strengths of krill; effects of phase variability on the distorted-wave Born approximation. ICES Journal of Marine Science, 60: 429−434.

Demer, D. A., and Conti, S. G. 2005. New target-strength model indicates more krill in the Southern Ocean. ICES Journal of Marine Science, 62: 25−32.

Demer, D. A., Conti, S., De Rosny, J., and Roux, P. 2003. Absolute measurements of total-target strength from reverberation in a cavity. Journal of the Acoustical Society of America, 113: 1387−1394.

Demer, D. A., and Martin, L. V. 1995. Zooplankton target strength: volumetric or areal dependence? Journal of the Acoustical Society of America, 98: 1111−1118.

Endo, Y. 1993. Orientation of Antarctic krill in an aquarium. Nippon Suisan Gakkaishi, 59: 465−468.

Foote, K. G. 1991. Summary of methods for determining fish target strength at ultrasonic frequencies. ICES Journal of Marine Science, 48: 211−217.

Foote, K. G., Everson, I., Watkins, J. L., and Bone, D. G. 1990. Target strengths of Antarctic krill (*Euphausia superba*) at 38 and 120 kHz. Journal of the Acoustical Society of America, 87: 16−24.

Greene, C. H., Stanton, T. K., Wiebe, P. H., and McClatchie, S. 1991. Acoustic estimates of Antarctic krill. Nature, 349: 110.

Hewitt, R. P., Watkins, J., Naganobu, M., Sushin, V., Brierley, A. S., Demer, D., Kasatkina, S., Takao, Y., Goss, C., Malyshko, A., Brandon, M., Kawaguchi, S., Siegel, V., Trathan, P., Emery, J., Everson, I., and Miller, D. 2004. Biomass of Antarctic krill in the Scotia Sea in January/February 2000 and its use in revising an estimate of precautionary yield. Deep-Sea Research Part II − Topical Studies in Oceanography, 51(12−13): 1215−1236.

Kils, U. 1981. The swimming behaviour, swimming performance and energy balance of Antarctic krill, *Euphausia superba*. BIOMASS Science Series, 3: 122.

McGehee, D. E., O'Driscoll, R. L., and Martin Traykovski, L. V. 1998. Effects of orientation on acoustic scattering from Antarctic krill at 120 kHz. Deep-Sea Research II, 45: 1273−1294.

Morris, D. J., Watkins, J. L., Ricketts, C., Buchholz, F., and Priddle, J. 1988. An assessment of the merits of length and weight measurements of Antarctic krill *Euphausia superba*. British Antarctic Survey Bulletin, 79: 27−50.

Ona E., 1999. Methodology for target-strength measurement. ICES Cooperative Research Report, 235.

de Rosny, J., and Roux, P. 2001. Multiple scattering in a reflecting cavity: application to fish counting in a tank. Journal of the Acoustical Society of America, 109: 2587−2597.

Stanton, T. K., Chu, D., Wiebe, P. H., Martin, L. V., and Eastwood, R. L. 1998. Sound scattering by several zooplankton groups. I. Experimental determination of dominant scattering mechanisms. Journal of the Acoustical Society of America, 103: 225−235.

Warren, J. D., Stanton, T. K., Benfield, M. C., Wiebe, P. H., Chu, D., and Sutor, M. 2001. *In situ* measurements of acoustic target strengths of gas-bearing siphonophores. ICES Journal of Marine Science, 58: 740−749.